

Absorption Coefficient of $\text{Bi}_2\text{Te}_{2.5}\text{Se}_{0.5}$ Structures Applicable to the Creation of Photoelectric Converters

Nuru Safarov^{1*}, Sevinc Orucova², Gurban Ahmadov³, Shahla Ahmadova³

¹ Department of Electronics and Telecommunications Engineering, Khazar University, Baku, Azerbaijan

² Azerbaijan Medical University, Baku, Azerbaijan

³ Institute of Physics of Azerbaijan Nas, Baku, Azerbaijan

Email Address

nsafarov@khazar.org (Nuru Safarov)

*Correspondence: nsafarov@khazar.org

Received: 12 December 2017; Accepted: 8 January 2018; Published: 14 February 2018

Abstract:

The dependences of the light absorption coefficient in the film structures $\text{Bi}_2\text{Te}_{2.5}\text{Se}_{0.5}$ on the photon energy have been experimentally studied. It is shown that the profiles of the distribution of selenium atoms over the thickness of the surface layer of unannealed and depleted thin $\text{Bi}_2\text{Te}_{2.5}\text{Se}_{0.5}$ films. It is also shown that the release of selenium during heat treatment is due to the relatively high vapor pressure of selenium in a three-component semiconductor compound. As a result of work are received $\text{Si} - \text{Bi}_2\text{Te}_{3-x}\text{Se}_x$ heterojunctions in thin-film execution, described by high values of differential resistance. Results of researches show, that the structures $\text{Bi}_2\text{Te}_{2.5}\text{Se}_{0.5}$ received by a method of discrete thermal evaporation in a uniform work cycle, are suitable for use in low-voltage devices.

Keywords:

Thin-Film Material, Semiconductor, Optical Properties, Crystal, Absorption Coefficient, Concentration

1. Introduction

The possibility of manufacturing various types of elements with heterojunctions using these compounds was proved. The $\text{Si} - \text{Bi}_2\text{Te}_{3-x}\text{Se}_x$ heterojunctions relate to the most promising structures that can be used to create photovoltaic converters stable for long-term operation, intended for large-scale energy production. Thin-film devices have very important properties, thanks to which the effective conversion of solar energy is feasible. Among the main optical properties of three-component $\text{Bi}_2\text{Te}_{3-x}\text{Se}_x$ compounds, the strongest absorption of light at energies exceeding the width of the forbidden band attracts the most attention. Extremely high values of the light absorption coefficient allow reducing the requirements for the quality of the material and reducing the cost of solar cells. So, for example, to create an absorbing layer of $\text{Bi}_2\text{Te}_{3-x}\text{Se}_x$, a film with a thickness of less than $1\mu\text{m}$ is sufficient, so that the issues

of the cost and availability of the material begin to play a less important role [1]. A sharp edge of absorption at energy of 1.54eV corresponds to direct inter band transitions.

2. Materials and Methods

2.1 Materials and Methods

The existence of a different absorption edge at lower energies is due to carrier transitions from the level associated with the *Bi* vacancy to the conduction band. In n-type films, the second absorption edge is not observed, which confirms the theory that hole conductivity is due to *Bi* vacancies [2-5]. $\text{Bi}_2\text{Te}_{3-x}\text{Se}_x$ heterojunctions were obtained by high-temperature annealing of samples. Breezy samples possessed straightening properties; the factor of straightening on occasions reached value 10^2 at displacement $0,2\text{V}$ and temperature 80K . Straightening character volt-ampere characteristic is kept down to temperature 300K . The control of the properties of the films directly in the process of their condensation makes it possible in a single technological cycle to form hetero structures with a given concentration of charge carriers. Films with the best parameters are obtained by spraying on a substrate at a temperature of $280\text{ }^\circ\text{C}$, followed by annealing for 25 minutes. The density of electrical energy removed from photo converters increases with increasing emitter temperature. Optical transitions from the valence band to the conduction band are possible only at levels located near and above the Fermi level. When introduced into the crystal of a large number of impurity centers of the energy levels corresponding to the impurity atoms are expanded to form an impurity band, which for small levels merges with the edge of the valence band, and the band gap is formed tail density of states and the Fermi level goes deep in the main zone.

$$g(E) = g_0(E)[f_v(E_v - E_F) - f_c(E_c - E_F)] \quad (1)$$

Where f_v and f_c - occupation probabilities of single-electron states; $g_0(E)$ - the density of the final states without regard to their amusement. From the main absorption spectra of heavily doped crystals with simple bands quantitative data on the number of equivalent ellipsoids in the zones can be obtained. Fundamental absorption spectrum in crystals with varying electron density, from minimum to maximum, it possible to determine the absolute value and position of extreme as the forbidden gap relative to each other [6-9]. Factors affecting the absorption in indirect transitions in heavily doped crystal, a scattering by impurities, which can inform the missing electron momentum he needs in indirect optical transitions [10]. For elastic scattering, the absorption coefficient is represented by the formula

$$\alpha(h\omega) = \frac{A_{dir}N_{dir}}{h\omega} (h\omega - E_{gl})^2 \quad (2)$$

Where N_{dir} - the concentration of impurity atoms, A_{dir} - a constant, E_{gl} - the width of the indirect gap for highly doped semiconductor selection rule does not make sense, because when the electron scattering by impurities significantly change its momentum. The formula for the total absorption of highly-doped crystal for indirect transitions taking into account the scattering by impurities in the energy $h\omega > (E_g + 4kT)$ takes the form

$$\alpha = \frac{A_{dir}N_{dir}+A}{h\omega} \left(h\omega - E_{gl} - \frac{Ak\theta}{A_{dir}N_{dir}+A} th \frac{\theta}{2T} \right)^2 \quad (3)$$

Which implies that the dependence $\sqrt{a\hbar\omega} = f(h\omega)$ is a straight line intersecting the axis of the energy at the point

$$h\omega = E_{gl} + \frac{Ak\theta}{A_{dir}N_{dir}+A} th \frac{\theta}{2T} \quad (4)$$

The volt–farads characteristics in an interval of temperatures 77–300K are investigated. With this purpose the structure $Bi_2Te_{2.5}Se_{0.5}$ also was mounted in vacuum cryostat, where furnace and the sensor of temperature were in a landing place of a sample. The temperature regulator provided maintenance of temperature with accuracy $\pm 1^{\circ}C$. With increase in temperature direct currents are limited to more high-resistance layers $Bi_2Te_{2.5}Se_{0.5}$ heterojunction, reverse currents grow more intensively and consequently at temperatures $T > 200K$ the factor of straightening appreciably decreases. At voltage more than 30mV straight lines volt–ampere characteristic are described by function of a kind $I = I_0 \exp(qV / \beta kT)$, with factor of ideality $\beta = 2-2, 5$ characteristic for a current, limited recombination's of carriers in a layer of a volumetric charge. The size β increases up to 3 at 100K. At the big voltage linear dependence $I(V)$ operates. The size diffusion's site of the volt – ampere characteristic in the field of the big currents makes 0,095–0,100V. With growth of temperature is higher 100K an inclination changes, and is lower 100K remains to constants, and at temperatures 77–100K initial sites of the volt–ampere characteristic is not described by expression $I = qSnd \exp[-q(V_{D_n} \cdot V)]$.

3. Results and Discussion

The position of which is shifted to shorter wavelengths with increasing concentration of impurities. Straight line depending also shifted towards lower energies with increasing concentration of impurities, and the slope increases. The conduction band of the $Bi_2Te_{2.5}Se_{0.5}$ has two minima, and the absolute minimum, four degenerate in the absence of external fields, is 0.18eV below the minimum in the center of the zone, so the study of the optical absorption spectra of strongly basic $Bi_2Te_{2.5}Se_{0.5}$ allows investigating changes in the doping of both at the same time lows [11–13]. The results of studies of the effect of heavy doping on the structure of the absorption curve associated with the direct inter-band transitions at 77K are shown in Figure 1. Samples $Bi_2Te_{2.5}Se_{0.5}$ was doped antimony and arsenic to a concentration of 10^{13} to $1.5 \times 10^{18} \text{ cm}^{-3}$. The thickness of the free samples was approximately 10 m. The figure shows that with increasing concentration of impurity centers exciting peak expanded, and then disappears. Absorption in $h\omega > E_g$ with increasing concentration and decreases to a value characteristic of a pure crystal without Coulomb interaction of carriers. The critical impurity concentration, at which the exciting absorption features in the spectrum disappear, turns out to be 10^{16} cm^{-3} . Spectra corresponding $N_D = 2 \times 10^{17}$ and $1,5 \times 10^{18} \text{ cm}^{-3}$ are in good agreement with the formula

$$\alpha(\omega) = A \frac{\sqrt{h\omega - E_g}}{h\omega} \quad (5)$$

which does not account for the interaction of electrons and holes. The intersection points of these lines with the axis of energy correspond to the band gap. Figure 1 show that with increasing impurity concentration the energy band gap is reduced. When the concentration of impurities is $1,5 \times 10^{18} \text{ cm}^{-3}$, $\Delta E = -1,1 \times 10^{-2} \text{ cm}^{-3} \text{ eV}$ in agreement with the value calculated the formula $\Delta E = -2 \left(\frac{3}{\pi}\right)^{1/3} \frac{e^2 N^{1/3}}{\epsilon}$. Direct 4 of

Figure 1 correspond to the case where the carriers injected into the light volume of the crystal [14].

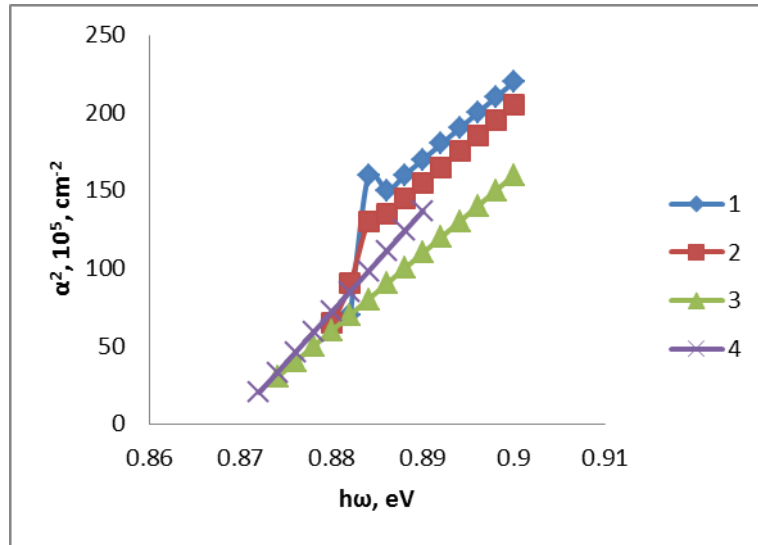


Figure 1. The effect of the concentration of impurities in the structure $Bi_2Te_{2.5}Se_{0.5}$ of the fundamental absorption edge concentrations: 1- $10^{13} cm^{-3}$; 2- $8 \times 10^{15} cm^{-3}$; 3- $2 \times 10^{18} cm^{-3}$; 4- light injection.

Figure 2 shows the absorption spectra of the main samples $Bi_2Te_{2.5}Se_{0.5}$ at 4.2K, more heavily doped with arsenic at a concentration of $5 \times 10^{18} cm^{-3}$ to $4 \times 10^{19} cm^{-3}$. It can be seen that the absorption edge associated with the direct inter band transitions is shifted toward longer wavelengths.

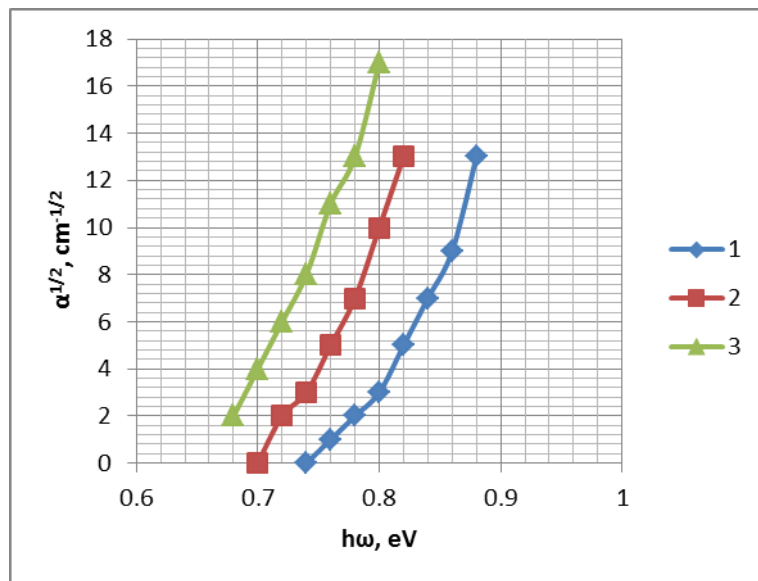


Figure 2. The spectra of the fundamental absorption edge $Bi_2Te_{2.5}Se_{0.5}$ heavily doped with phosphorus, arsenic and gallium: 1 pure; 2- $2 \times 10^{19} cm^{-3} (P)$; 3- $10^{19} cm^{-3} (As+Ga)$.

For a more detailed analysis of weak absorption, in Figure 2 the experimental data for samples $Bi_2Te_{2.5}Se_{0.5}$ with impurity atoms phosphorus, arsenic and gallium obtained at 80K, built to scale $\sqrt{\alpha(\omega)} \sim h\omega$. The same figure also shows the spectrum of a pure sample. The concentration of impurities in pure sample $10^{13} cm^{-3}$ (figure 2. 1). The impurity concentration of phosphorus atoms in the

sample $2,4 \times 10^{18} - 4,3 \times 10^{19} \text{ cm}^{-3}$ (figure 2. 2). The impurity concentration of arsenic and gallium atoms in the sample, respectively, equal to $2,9 \times 10^{19} \text{ cm}^{-3}$; $1,8 \times 10^{19} \text{ cm}^{-3}$ (figure 2. 3). The figure shows two features: 1) absorption of highly doped uncompensated samples more sharply depends on the photon energy than pure sample; 2) absorption of all compensated samples begins at about the same photon energy, while at the beginning of the compensated sample absorption is shifted toward longer wavelengths. This indicates a significant reduction in band gap doped. For example, for sample 2 band gap decreased 80 meV . Reducing proportional to the cube root of the total concentration of impurity atoms and does not depend on the electron concentration.

$$\Delta E_g \sim \sqrt[3]{(N_D + N_A)} \quad (6)$$

Temperature dependence of a current on a voltage is much weaker, than it is necessary to expect from generations–recombination's model. In this case Fermi's levels lay in a band of conductivity and in a valence band accordingly for $\text{Si-Bi}_2\text{Te}_{3-x}\text{Se}_x$. Weak temperature dependence of a direct current, constancy dI/dV at change of temperature and great value of a current of saturation specifies such opportunity. At high temperatures the tunnel current also exists. At higher temperatures ($200\text{-}300\text{K}$), prevailing become activity processes. The inclination an exponential site became temperature-dependent, experimental points well to be lying on straight lines in coordinates $\ln I \cong T^{-1}$. Proceeding from the tunnel mechanism of carry of a current, in double logarithmic scale dependence of a current on a voltage can look as sedate. At small displacement ($20\text{-}30\text{mV}$) reverse branches submit to the sedate dependence, which can be connected to presence of superficial outflow or the complex mechanism of tunneling [15, 16]. From temperature dependence of a reverse current it is possible to draw a conclusion, that in the field of temperatures $100\text{-}200\text{K}$ course of a current is defined by a generation's current, since at voltage $30\text{-}200\text{mV}$ the reverse current has the sedate dependence close to $kI \cong V^n$, ($n \approx \frac{1}{2}$) which is characteristic for a generation's current for a case of sharp transition.

As the reverse current with growth of a voltage changes under the reverse law $I_{\text{opp}} \cong \sqrt{V}$, at $30\text{-}130\text{mV}$ direct displacement the direct current is described by dependence $I = I_0 \exp(qV / \beta kT)$, where $\beta \sim 2$. Thus, it is possible to conclude, that in an interval $77\text{-}130\text{K}$ at $V_{\text{direct}} = 20\text{-}130\text{mV}$ and $V_{\text{reverse}} = 40\text{-}120\text{mV}$. Thus the reverse current through transition is basically generations. At temperatures from above 200K , the exponent becomes more than 1. Measurement of capacity p-n transition depending on a voltage allows to determine such major parameters, as the width of area of a volumetric charge, diffusion potential, concentration of acceptors and donors in the field of a volumetric charge, structure of a locking layer, the mechanism of straightening. Results of measurements testify to sharpness of transition of the volt - farad characteristic resulted on figure 3.

As is known for a barrier the metal - semiconductor, as well as for sharp asymmetrical transition, the width of the impoverished layer is expressed by the following formula

$$W = \sqrt{2\varepsilon_s(V_B - V - kT)q / N_d} \quad (7)$$

The specific capacity of the impoverished layer is defined by the formula

$$C = \sqrt{q\epsilon_s N_d (2(V_B - V - kT)q)} \quad (8)$$

Whence

$$N_d = (2/q\epsilon_s) \left[-1 / \left(d\left(\frac{1}{C^2}\right) / dV \right) \right] \quad (9)$$

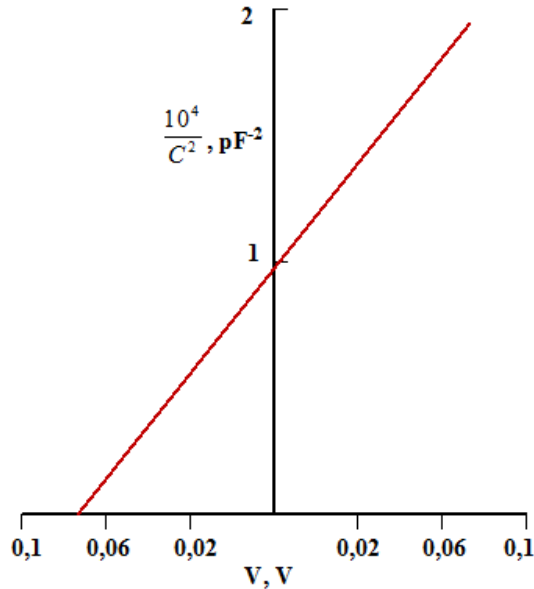


Figure 3. The volt - farad characteristic of structure $Si - Bi_2Te_{3-x}Se_x$.

The schedule of dependence on negative voltage is constructed. Apparently from figure 3 dependence $C^{-2} \cong V$ has linear character up to $0,1V$. Concentration ionized centers N_d in a barrier, determined on an inclination $C^{-2} \cong V$ makes $4 \cdot 10^{15} cm^{-3}$. The diffusion potential determined by extrapolation of resulted dependence is equal $\sim 0,08-0,09V$. Influence of an intermediate layer on capacity is in details analyzed on the basis of Bardin's model [17]. At presence of a thin high-resistance layer by superficial charges on border undressed dependence C^{-2} from $V_{reverse}$ remains still linear with an inclination $2/q\epsilon N_d$, as well as for the diode without an intermediate layer, but the point of crossing of this dependence with axis $V_{reverse}$ is displaced aside higher values. In the major parameter describing qualitatively made structures, the size of differential resistance is at zero displacement. The experimental points reflecting dependence of differential resistance at zero displacement from temperature are shown on figure 4. Apparently, the resulted dependence submits to the exponential law in an interval of temperatures $77-200K$, and at high temperatures dependence amplifies.

As a result of work are received $Si - Bi_2Te_{3-x}Se_x$ heterojunctions in thin-film execution, described by high values of differential resistance. Results of researches show, that film p-n the structures received by a method of discrete thermal evaporation in a uniform work cycle, are suitable for use in low-voltage devices.

In Figures 5 and 6 show typical dependences of the absorption coefficient α and the parameter $(\alpha h\nu)^2$ on the photon energy for single-crystal and thin-film $Bi_2Te_{3-x}Se_x$ samples. When approaching the absorption edge both in thin films and in crystals, a sharp change occurs, typical of semiconductors with direct inter band transitions. At energies greater than the width of the band gap, α exceeds $10^7 m^{-1}$. For several thin

films, the values $\alpha=5*10^7 - 6*10^7 m^{-1}$ were obtained. They are the maximum among published values of α for any semiconductors, which agrees with very high short-circuit current densities ($390A/m^2$), typical for effective solar cells based on $Si - Bi_2Te_3 - xSe_x$ [18-21].

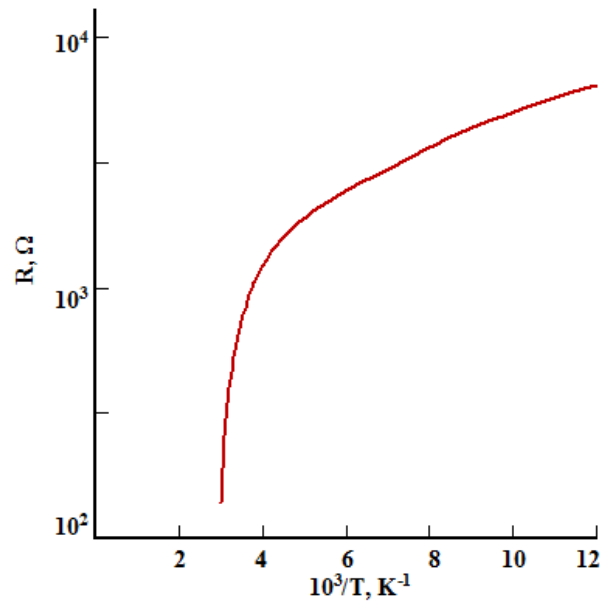


Figure 4. Temperature dependence of differential resistance at zero displacement.

The displacement of the curves of the dependence $\alpha(h\nu)$ along the energy axis corresponds to the data of other scientific papers. In most thin films, the edge of the main absorption band corresponds to energy approximately equal to $1.02eV$, and in single crystals $0.95-0.96eV$. This can be due to several reasons. First, there is an electric field at the grain boundaries in polycrystalline materials. The absorbing properties of the material change under the influence of this field. However, this effect is usually observed for small values of α in the tail region of the spectral characteristic $\alpha(h\nu)$. Therefore, it is unlikely that it is the main reason for the displacement of these characteristics relative to each other. Secondly, different samples of single crystals and thin films have a different chemical composition. After annealing the thin films in an inert atmosphere (Figures 5 and 7), the curves $\alpha(h\nu)$ are shifted to that energy region where analogous characteristics of single crystals are located. The effect of temperature on the spectral characteristics of the absorption coefficient is illustrated in figure 5. When the temperature drops to $100K$, the edge of the optical absorption corresponds to higher photon energy than its value at room temperature. The presence of a shift in the edge of the absorption band does not contradict the results of measurements of the temperature dependence of the band gap. For the allowed direct interband transitions, the following relation between the absorption coefficient and the photon energy is valid:

$$\alpha h\nu = A(h\nu - E_g)^{1/2} \quad (10)$$

Here A is a constant, and E_g is the width of the forbidden band. Thus, for semiconductors in which the absorption of light is accompanied by direct inter band transitions, the dependence $(\alpha h\nu)^2$ on $(h\nu)$ has the form of a straight line. The position of its intersection with the photon energy axis characterizes the width of the forbidden band. At room temperature, single crystals and thin films (Figure 6) are semiconductors with a direct band gap, whose width is 0.966 and $1.02eV$, respectively.

At a temperature of $100K$, the width of the forbidden band of thin-film material increases than predicted by the theory, and reaches $1.04eV$. However, the most important circumstance is that the above dependences of the absorption coefficient on the photon energy indicate the existence of direct inter band transitions.

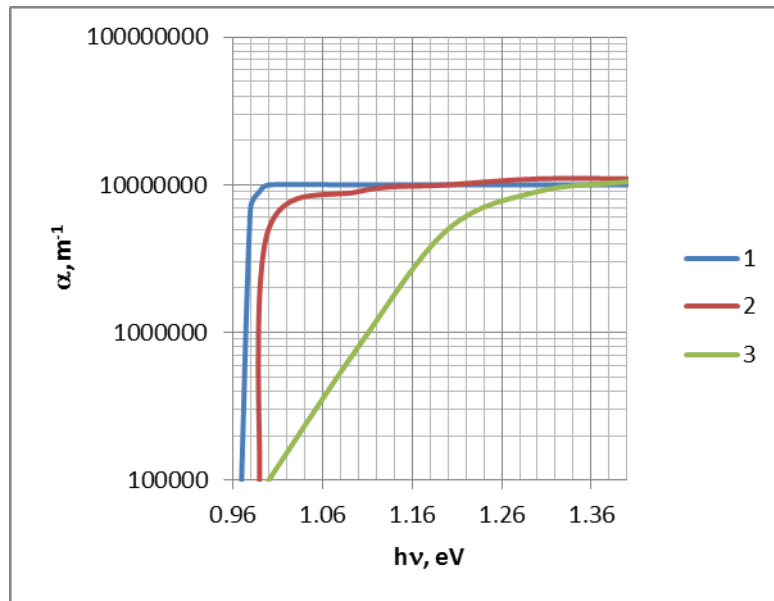


Figure 5. Dependences of the absorption coefficient α on the photon energy in Bi_2Te_3 - xSe_x single crystals at a temperature of $300K$ (1) and $100K$ (2), as well as in thin films at $300K$ (3).

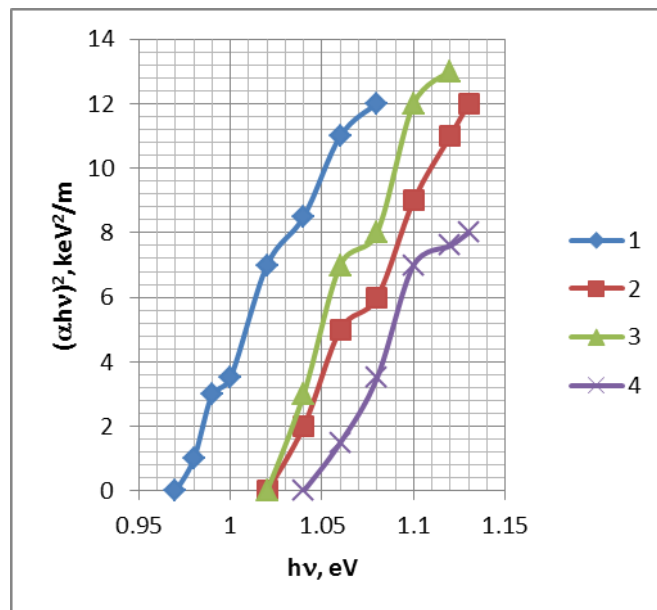


Figure 6. Dependence of the parameter $(\alpha h\nu)^2$ on the photon energy for various samples of $Bi_2Te_{3-x}Se_x$.

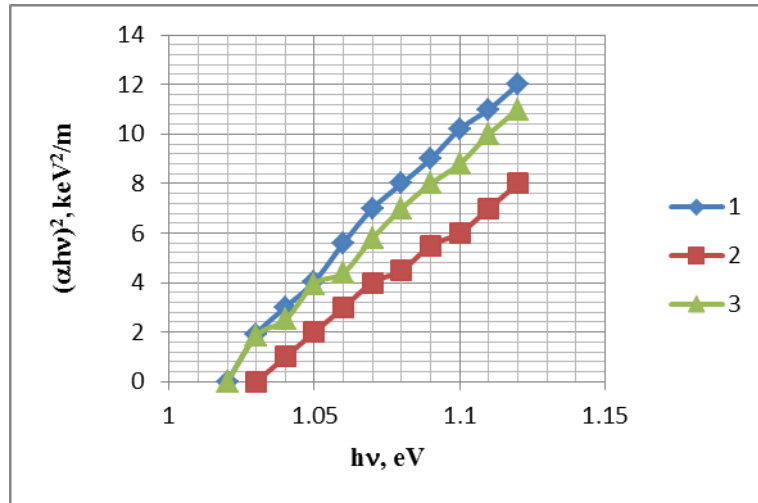


Figure 7. The effect of annealing on the dependence of the parameter on the photon energy. 1 - annealing with oxygen at a temperature of 200 °C; 2 - annealing in high vacuum at 220 °C; 3 - unshrouded thin film.

Tails of the spectral characteristics of the absorption coefficient at small α are observed both in single crystals and in thin films [22-24]. In these regions, the dependence of α on $h\nu$ is not described by equation (11). If interband transitions occur with the participation of phonons, then it takes the form.

$$\alpha = A(h\nu - E_g + E_p)^2 / (\exp(E_p/kT) - 1) \quad (11)$$

Here A is a parameter that does not depend on the photon energy, E_p is the phonon energy, and E_g is the width of the forbidden band for indirect transitions. The energies corresponding to the points of their intersection with the abscissa axis are consistent with the previously reported values of the wave number typical of optical phonons. The energy values found by these authors are 0.019; 0.028; 0.048 and 0.058 eV correspond to wave numbers that are characteristic of optical phonons. The absence of transitions at a low temperature (10K) also confirms that additional absorption of low-energy radiation is associated with transitions in which phonons participate. The influence of heat treatment can be judged from the data presented in Figure 6. Annealing in oxygen at a temperature of 200 °C for 10 min leads to a slight increase in the absorption coefficient at any photon energy, i.e., to an increase in the absorptivity of $Bi_2Te_{3-x}Se_x$. This change in α is not associated with the growth of an oxide or any other surface film, since in the samples from the surface of which the oxide layer was removed by ion etching just before the measurement of the absorption coefficient, the values of α also increased. In deliberately oxidized samples, no such effect was observed. The thickness of the oxide layer, formed because of annealing at 200 °C in pure oxygen, is usually 5 ... 6 nm. After annealing the films, the slope of the curves of $(\alpha h\nu)^2$ versus $h\nu$ becomes approximately the same as in single crystals, probably due to an increase in the degree of homogeneity of the composition both over the thickness and along the film. An analysis of the composition by the method of spectroscopy shows that the degree of heterogeneity in the distribution of atoms is reduced to below 0.2%. The effect of heat treatment is illustrated in figure 7. The dashed line corresponds to the original unannealed thin film. After heat treatment in oxygen, the absorption coefficient increases. The difference between the results, which lead to these two types of heat treatment, is insignificant. This is confirmed by the same increase in the short-circuit

current of heterojunctions. However, heating the samples in a high vacuum causes a decrease in the absorption coefficient.

An investigation of films annealed in this way by the method of spectroscopy indicates the presence of a significant gradient of the concentration of selenium near the surface. The profile of the distribution of the concentration of selenium in depth, obtained by this method, is shown in figure 8.

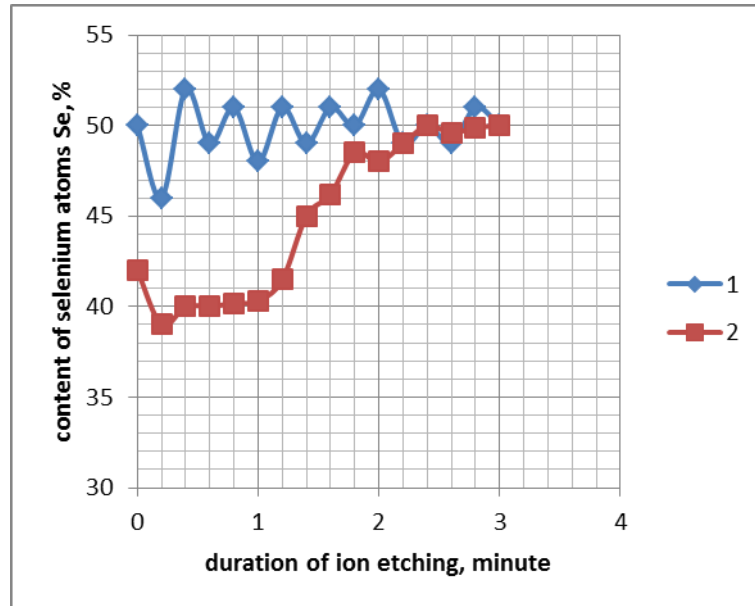


Figure 8. The profiles of the distribution of selenium atoms in the thickness of the surface layer unblended (1) and measured in vacuum at 200°C for 10min (2) thin films of $Bi_2Te_{3-x}Se_x$.

4. Conclusions

The release of selenium during the heat treatment is probably due to the relatively high vapor pressure of *Se* in the three-component compound. Consequently, the change in the absorption coefficient is associated in this case with significant variations in the composition of the films.

Absorption of highly doped uncompensated samples more sharply depends on the photon energy than pure sample. Absorption of all compensated samples begins at about the same photon energy, while at the beginning of the compensated sample absorption is shifted toward longer wavelengths. The energy gap for direct and indirect inter-band transitions approximately equally dependent on the total concentration of donors and acceptors in the crystal $Bi_2Te_{3-x}Se_x$ in the range $10^{18} - 5 \times 10^{19} \text{ cm}^{-3}$. Thanks to the successful development of solar cells based on $Bi_2Te_{3-x}Se_x$, the other three-component *Si* - $Bi_2Te_{3-x}Se_x$ compounds attract so much attention. Great interest in these semiconductors can contribute to their wider use as materials for the creation of photoelectric detectors and converters. Studies on the improvement of *Si* - $Bi_2Te_{3-x}Se_x$ heterojunctions due to their undoubted potential capabilities will be sold.

Conflicts of Interest

The authors declare that there is no conflict of interest regarding the publication of this article.

References

- [1] Gurban Axmedov. Methods for Determination of the Optical Constants of the Substance BiTe-BiSe, American Journal of Physics and Applications. Vol. 2, No. 6, 2014, pp. 150-155. doi: 10.11648/j.ajpa.20140206.16.
- [2] Werner, J.H., Mattheis, J., and Rau, U. (2005) Efficiency limitations of polycrystalline thin film solar cells: case of Cu(In,Ga)Se₂. Thin Solid Films, 480/481, 399–409.
- [3] MusaverMusayev, SedreddinAxmedov, GurbanAxmedov. Physical Properties and Influence of the Tempering on Electric Properties Films Bi₂Te₃, International Journal of Materials Science and Applications. Vol. 3, No. 3, 2014, pp. 111-115. doi: 10.11648/j.ijmsa.20140303.17.
- [4] N Safarov, G Axmedov, S Axmedov. Investigations of Mathematical Models in SolarCollectors. American Journal of Energy Engineering. 2 (3), 75-79. 2014.
- [5] AA Bayramov, AM Hashimov, NA Safarov, GM Akhmedov. Thermophotovoltaic Solar Energy Converters on the Basis AVBVI. 2006 IEEE 4th World Conference on Photovoltaic Energy Conference. Volume 1. 2006/5, pp.651-654.
- [6] J. Pankove, P. Algrain. Optical absorption of arsenic – doped degenerate germanium. Phys. Rev.126, 1962, 956.
- [7] A.A.Rogachev. Reducing the semiconductor bandgap with strong doping, FTT, 9, 1967, 369.
- [8] Tatarinova L. The structure of amorphous solid and liquid substances. (Moscow: Nauka, 1983, 151p.)
- [9] Nabitovich I., StechievYa, VolosukYa. Defining a coherent intensity and the background intensity on the experimental curve of electron scattering. Crystallography, (1967), v.12, no 4, pp.584-590.
- [10] Lifei Yu, Dechun Li *, Shengzhi Zhao, Guiqiu Li and Kejian Yang. First Principles Study on Electronic Structure and Optical Properties of Ternary GaAs:Bi Alloy. Materials 2012, 5, 2486-2497; doi:10.3390/ma5122486.
- [11] G. Axmedov. Phase formation in bite nanofilms and crystallization of Bi₂Te₃ (Se₃) nanothickness amorphous film. Scientific Israel – technological advantages, Vol.14, 2012, No.4 p.85-94.
- [12] G. Axmedov. Kinetic of phase transformations of Bi₂Se₃ nano-thickness films. Scientific Israel – technological advantages, Vol.13, 2011, No.4 s.57-62.
- [13] G. K. Chadha. Semimetal-semiconductor transition in Bi-In system. Indian Journal of Pure & Applied Physics. Vol.40, June 2002, pp. 407-416.
- [14] Boqolyubov N. Problems of dynamical theory in statistical physics. Moscow: Gostekhizdat, , 1946, 359p.
- [15] M. Saranya , C. Santhosh , S. Prathap Augustine & A. Nirmala Grace (2014) Synthesis and characterisation of CuS nanomaterials using hydrothermal route, Journal of Experimental Nanoscience, 9:4, 329-336, DOI: 10.1080/17458080.2012.661471.

- [16] X A Fan, J Y Yang¹, W Zhu, S Q Bao, X K Duan, C J Xiao, Q Q Zhang and Z Xie. Effect of nominal Sb₂Te₃ content on thermoelectric properties of p-type (Bi₂Te₃)_x(Sb₂Te₃)_{1-x} alloys by MA-HP 2006 J. Phys. D: Appl. Phys. 39 5069.
- [17] C. Kastl, T. Guan, X. Y. He, K. H. Wu, Y. Q. Li and A. W. Holleitner. Local photocurrent generation in thin films of the topological insulator Bi₂Se₃Bi₂Se₃. Appl. Phys. Lett. 101, 251110 (2012); <https://doi.org/10.1063/1.4772547>.
- [18] Gurban Akhmedov. Physical and Optical Properties of the Films Bi₂Te₃-Bi₂Se₃. Journal of Advances in Physics. Vol 11 No 2. 3017-3022 (2015).
- [19] G Abdullaev, M Bakirov, N Safarov. Silicon solar cells with antireflection layers of silicon oxide and nitride. Applied solar energy, Volume 29. Issue 1. pages 76-78. 1993.
- [20] Nuru Safarov. Polymer - Silicon Sensor for Determination Flow. Global Journal of Engineering Science and Research Management. 3(9): September 2016, pp.19-21.
- [21] N. A. Safarov, F.N. Tatardar, S. S. Amirov. The hybride composites based new materials for the Electromechanical and acoustico-electrical converters. Journal of non-oxide glasses vol. 9, no 1, 2017, p. 19 – 23.
- [22] Shimakawa, S. et al. Characterization of Cu(In,Ga)Se₂ thin films by time-resolved photoluminescence. Phys. Status Solidi A, 203(11), 2630(2006).
- [23] Evan B. Pollock and Robert J. Lad. Influence of dosing sequence and film thickness on structure and resistivity of Al-ZnO films grown by atomic layer deposition. Journal of Vacuum Science & Technology A: Vacuum, Surfaces, and Films 32, 041516 (2014).
- [24] Ishu Sharma, Pawan Kumar, S.K. Tripathi. Physical and optical properties of bulk and thin films of a-Ge-Sb-Te lone-pair semiconductors. Phase Transitions. Volume 90, - Issue 7. Pages 653-671 (2017). <https://doi.org/10.1080/01411594.2016.1260720>



© 2018 by the author(s); licensee International Technology and Science Publications (ITS), this work for open access publication is under the Creative Commons Attribution International License (CC BY 4.0). (<http://creativecommons.org/licenses/by/4.0/>)